Continuous thermal monitoring of the 2008 eruptions at Showa crater of Sakurajima volcano, Japan

Akihiko Yokoo*

Sakurajima Volcano Research Center, Disaster Prevention Research Institute, Kyoto University, 1722-19 Sakurajima-Yokoyamacho, Kagoshima 891–1419, Japan

(Received June 10, 2009; Revised August 18, 2009; Accepted August 31, 2009; Online published January 18, 2010)

An infrared thermal monitoring system installed 3.5 km from the Showa crater of Sakurajima volcano, Japan, enabled the capture of continuous thermal waveform data at 1 Hz during two recent episodes of eruptive activity. The eruptions were characterized by a sudden increase in volcanic cloud temperature in the first 2–5 s, followed by gradual cooling over a few minutes. The maximum cloud temperature varied widely between individual events with a range of more than 180°C. A positive relation between the maximum temperature and the exit velocity of the cloud has also been established. At higher temperatures and faster exit velocities of the volcanic cloud, the eruptions tend to be accompanied by pyroclastic density currents. However, no strong correlation was observed in a 6-month period of 2008 between temporal changes in surface manifestation of eruptive activity and the change of cloud temperatures. Identification of factors that control such observed apparent temperatures of volcanic cloud would lead to a better understanding of the thermodynamics of the eruption itself.

Key words: Infrared thermal observation, Sakurajima volcano, Showa crater, the 2008 eruptions, radiative thermal energy.

1. Introduction

Eruptions at the Showa crater on the southeastern flank of Sakurajima volcano in Japan (Fig. 1) started again in June 2006 after 58 years of dormancy. From 2006 to the end of 2008, four episodic eruptions had occurred: June 2006 (ca. 2 weeks), May–July 2007 (ca. 6 weeks), February 2008 (4 days), and April–October 2008 (ca. 26 weeks). Ground-based thermal observations for the area around the Showa crater were conducted in the 3 months prior to the first eruption in 2006 (Yokoo *et al*., 2007). Compared to a survey conducted in 1992 (Kamo *et al*., 1995), elevated geothermal activity indicating an increase in volcanic activity in the vicinity of the crater was observed preceding the first eruption at the Showa crater, while there were no notable changes in the seismic and geodetic records. Geothermal changes monitored even at a distance of 2–4.5 km, therefore, appear to have been the only significant precursor signals of the reactivation of this crater. Remote geothermal monitoring, conducted not only from the ground but also from the air, and even space, may thus be particularly useful for detecting imminent eruptions at dormant volcanoes, as in the 2004 eruption of Asama volcano (Kaneko *et al*., 2006).

During the second eruption episode in 2007, apparent temperatures of volcanic clouds were measured using an infrared thermal imaging camera from the eastern foot of the Sakurajima volcano (the Kurokami Observatory; Fig. 1). Based on 14 measurements taken over 6 weeks along with the results of infrasound-movie observations (Yokoo *et al*., 2008b), the activity of this eruption episode was divided into the following three stages. The first stage was characterized by the ejection of volcanic materials with an apparent temperature of 40–60°C, suggesting the ejection of choking materials within the conduit, which was reopened during the main stage of the eruption. The second, and main, stage was characterized by repeated explosive eruptions, accompanied by impulsive infrasound waves, with cloud temperatures reaching 100–160°C. Volcanic glow and incandescent ejecta were occasionally observed during this eruption stage. In the final stage, the eruptions began to ease, and the eruption cloud temperature dropped to 20–30°C and were accompanied by minor ash emissions with monotonic infrasound waves. The low temperatures at this stage were found to be similar to those for fumarolic steam venting in the vicinity of the crater.

However, there is some uncertainty in the interpretation of the 2007 thermal observations related to the progress of eruptive activity. The temporal change in volcanic cloud temperature was measured only 14 times over the 6-week observation period, while more than 578 individual eruptions were visually confirmed over the same period (Yokoo *et al*., 2008b). Additionally, the first 7 thermal measurements were made based on a small number of single shots, which may not adequately account for the wide temporal variations in the thermal waveforms of the eruption cloud, particularly at the beginning of the eruption (e.g., Sahetapy-Engel *et al*., 2008). After recognizing this issue, the thermal waveforms were recorded at an 1-Hz sampling rate for the

*Present affiliation: Department of Geophysics, Graduate School of Science, Tohoku University, Aramaki-Aza-Aoba 6-3, Aoba-ku, Sendai 980-8578, Japan.

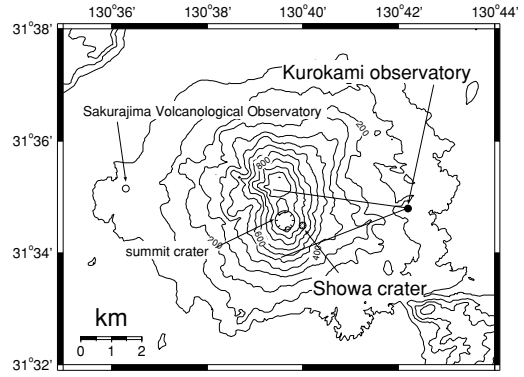

Fig. 1. Map of the Sakurajima volcano showing the Kurokami Observatory and the Showa crater. The field-of-view of the infrared thermal camera at the observatory is indicated.

remaining 7 observations. Although these high frequency observations would be preferable for considering the thermodynamics of each eruptive event, these are not suitable thermal data for investigating the temporal changes in eruptive activity during an episode. In order to properly consider this issue, continuous observations from permanent stations are also needed.

In recent years, continuous field observations of the thermal characteristics of volcanic eruptions have been attempted at a number of volcanoes (Harris *et al*., 2003; Johnson *et al*., 2004; Ripepe *et al*., 2005; Patrick *et al*., 2007), and several types of sensors have been employed, including a spot-targeting infrared thermometer and an infrared thermal imaging camera. Most of these observations have been conducted over periods of a few hours or days, and there are very few reports of permanent observation stations collecting data suitable for comparing and investigating changes in volcanic activity at time scales of weeks to months. Although Stevenson and Varley (2008) conducted long-term observations of the temperature of fumaroles around the crater of the Volcán de Colima, Mexico, there is very little data on volcanic plume temperature.

In this study, a new 24-h continuous thermal monitoring system was installed to observe the Sakurajima volcano. This system was operational during the 2008 eruptions of the Showa crater, and the collected data enabled investigation of the thermal characteristics. Moreover, thermal energy radiated during some eruption periods was estimated for tentative utilization of the obtained continuous thermal data.

2. Thermal Monitoring System at Sakurajima Volcano

In August 2007, approximately 6 months before the most recent eruption episode that started in April 2008, an infrared thermal imaging camera (TH7102MV, NEC-Sanei) was installed at the Kurokami Observatory with a clear line of sight of the Showa crater located 3.5 km to the east (Fig. 1). The main purposes of installing a system with this camera was to continuously record thermal data on volcanic clouds produced during the eruptions and to track the temporal variation in ground surface temperature in areas around the crater, which was known to have exhibited geothermal anomalies preceding the 2006 eruptions (Yokoo *et al*., 2007). Similar infrared imaging camera systems for continuous monitoring of thermal activity over a period of several years have been reported by Chiodini *et al*. (2007) for an Italian hydrothermal area, and by Stevenson and Varley (2008) targeting fumaroles of the Volcán de Colima.

The thermal camera deployed at Sakurajima is sensitive to infrared light in the 8–14 μm wavelength range. The camera is set in a waterproof housing outside the observatory, and it is aimed at the volcano through a ZnSe window that is transparent at infrared wavelengths. The sampling frequency of thermal data capture was set to 1 Hz, and the obtained images were 320×240 pixels in size, covering a field of view (FOV) of H29°×V22° with an instantaneous field of view (iFOV) of 1.58 mrad (Fig. 2). At a distance of 3.5 km, the iFOV equates to a measurement area of 5.53 m in diameter (30.58 m^2), which is sufficiently small compared to the diameter of the crater (ca. 180 m). Only a square zone (24×24 pixels) including the Showa crater was selected in the present analysis (Fig. 2(a)) in order to exclude plume dynamics of eruption clouds, such as cooling during ascent, which is extraneous to the aims of the present study.

The temperature range measured by this system is 0–250°C (occasionally, −20–110°C). Although a higher range (of 100–800°C) is available, it is not sufficiently sensitive for monitoring temperatures less than 100°C, which are of particular interest because it is crucial to monitor thermal activity under both dormant and active eruption conditions at the Sakurajima volcano.

The camera is controlled automatically and the data are logged by a computer inside the observatory. Re-sampled data at 10-s intervals are transmitted to the Sakurajima Volcanological Observatory on the opposite (west) side of the volcano (Fig. 1) via dedicated telephone lines, allowing remote semi-real-time monitoring. The performance of the system has been reported in detail by Yokoo *et al*. (2008a).

3. Eruptions at Showa Crater in 2008

In 2008, the Showa crater erupted more energetically and frequently than in the two previous episodes in 2006 and 2007. During the third episode of eruptions (February 3–6, 2008), quite explosive eruptions accompanied by dense pyroclastic density currents (PDCs), reaching distances of up to 1.5 km from the crater, were observed (Fig. 3(a)). The peak amplitudes of infrasound waves associated with these eruptions were recorded as 80–150 Pa at a station 2.3 km from the crater. These values of infrasound amplitudes are similar to those of the recent Vulcanian eruptions that occurred at the summit crater (Yokoo *et al*., 2009). This episode lasted for only four days, with sudden onset and cessation.

In the first 10 weeks of the fourth eruption episode (the latest period), which began on April 3 after a hiatus of 2 months, two types of eruptions occurred almost daily: an eruption accompanied by impulsive infrasound waves and incandescent ejecta, and an intermittent, quiet venting of ash similar to the eruptions in 2006 and 2007. The mean eruption duration was approximately 14 min for 839 eruptions identifiable from daytime video monitoring at the Kurokami Observatory (the different eruption types were not distinguished for these durations). The longest erup-

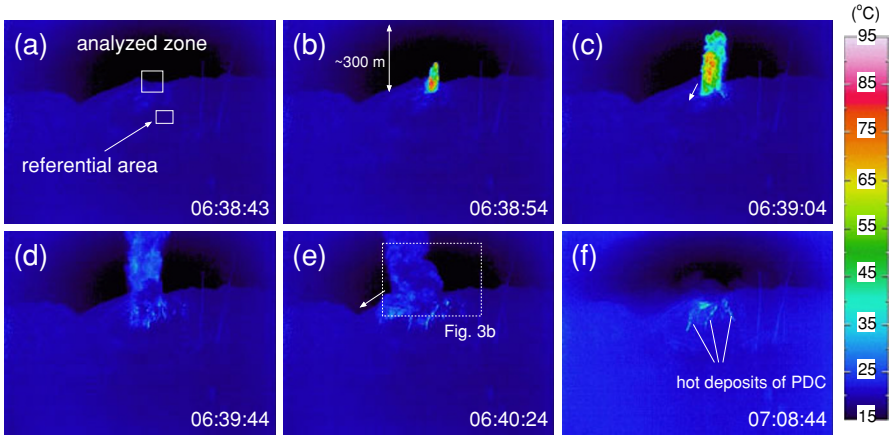

Fig. 2. Thermal snapshots of the eruption at the Showa crater on May 7, 2008. (a) 1 s before the eruption, and (b) 10 s, (c) 20 s, (d) 60 s, (e) 100 s, and (f) 30 min after the onset of the eruption (time data are superimposed at the lower right of each image). Square zones in (a) denote the areas analyzed for extraction of the apparent temperature of the volcanic cloud and for reference, respectively. Arrows in (c) and (e) denote the flow directions of pyroclastic density currents (PDCs), the deposits of which can be seen in several valleys on the frontal flank in (f). The broken line denotes the FOV shown in Fig. 3(b).

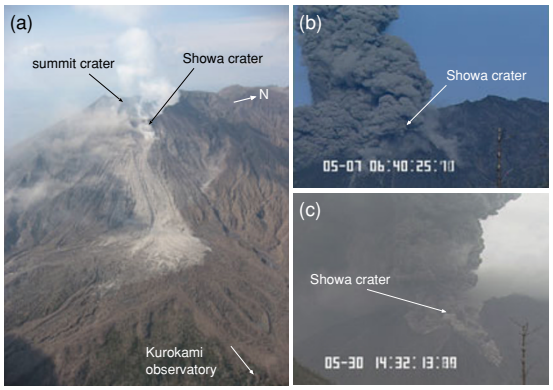

Fig. 3. (a) Distribution of deposits of one of the most vigorous PDCs on February 6, 2008. Photograph was taken by T. Takayama from a helicopter 1.5 h after the eruption. (b, c) Typical PDC flowing down the southern flank of the Sakurajima volcano and along the valley. Images were acquired using a TV camera installed at the Kurokami Observatory (Fig. 1) with the support of the Japan Broadcast Association (NHK).

tive single event lasted more than 5 h with continuous ash emissions on April 23. A total of 33 small PDCs caused by the partial collapse of volcanic clouds or by overflow directly from the crater were observed during this fourth episode, similar to the previous episodes (Fig. 3; Yokoo *et al*., 2008b). Volcanic glow was observed frequently from April until early June. Near the end of this period of volcanic glow (June 9–13), explosive eruptions accompanied by 20–50 Pa infrasound waves were pronounced, whereas amplitudes of infrasound waves of almost all eruptions observed before June were only a few Pascals or less. After June 2008, eruptive activity decreased abruptly, and eruptions occurred sporadically every 8–28 days. Ash ejections finally ceased on October 20, 2008.

Contrary to our expectation based on the pre-2006 case (Yokoo *et al*., 2007), obvious precursory signals in ground surface temperature around Showa crater exceeding diurnal and seasonal changes of variations cloud not identified before neither the third nor the fourth eruption episodes. It would be because geothermal activity around the crater already had become considerably high before the first episodic eruptions in 2006 and such condition had continued to those dates.

4. Thermal Data

During the 2008 eruption episodes, particularly for those after April, continuous thermal data were successfully recorded by the new monitoring system, even at night when video monitoring systems using high-sensitivity TV cameras (Yokoo *et al*., 2009) are ineffective. A total of 808 thermal events were recorded (Figs. 2 and 4), although some events were missed due to adverse weather conditions.

The maximum apparent surface temperature of volcanic clouds for each eruptive event was determined from the obtained thermal data. The highest temperature on February 6 in association with a vigorous PDC eruption event (Fig. 3(a)) exceeded the maximum scale of the thermal sensor (>250°C) and was recorded as an over-scale reading. Cloud temperatures for other cases were within in the range of 16–203°C (Fig. 4(a)), which was not as high as those observed at other active volcanoes (Harris *et al*., 2003; Ripepe *et al*., 2005) and can be attributable to the relatively long distance between the camera and the crater (c.f., Harris *et al*., 2009). These observations were affected by a combination of high atmospheric transmissivity along with the propagation path of infrared light, and the coarse spatial resolution of the camera compared to the sizes of the hot particles ejected. More than 85% of the event data for the surface temperature of volcanic clouds is below 50°C. The average temperature of 39°C (median temperature 33°C), is higher than that reported for the last stage of the 2007 eruptions (Yokoo *et al*., 2008b), and slightly lower than that for the first stage of the 2007 events.

Exit velocities of the volcanic clouds at the crater rim, which were estimated from good video images by tracing the heads of clouds for the first 10–30 frames (0.3–1.0 s), are plotted against their maximum temperatures in Fig. 4(b). A positive, but weak, correlation among them may be recognized. PDCs tended to accompany the eruption events with volcanic clouds of higher temperatures that had higher

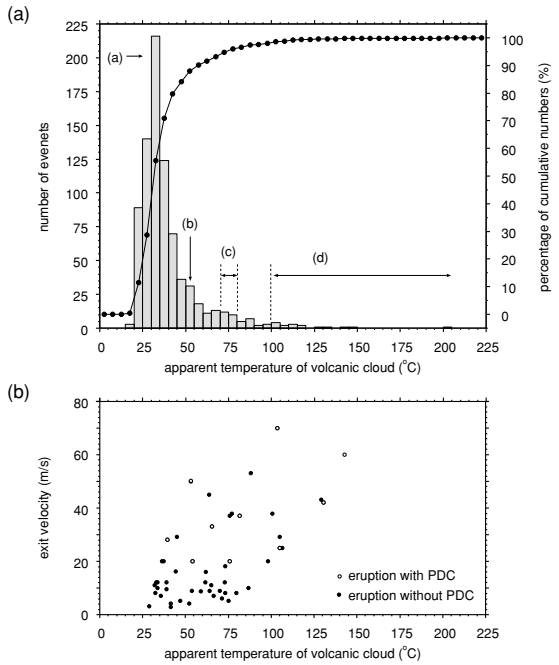

Fig. 4. (a) Histogram of maximum apparent temperature for each eruption cloud. Thermal waveforms for events in selected temperature ranges (a to d) are displayed in Fig. 5. (b) Relation between maximum temperature of volcanic cloud and its exit velocity at the crater (55 events). The 10 white circles denote events with PDCs out of 55 events.

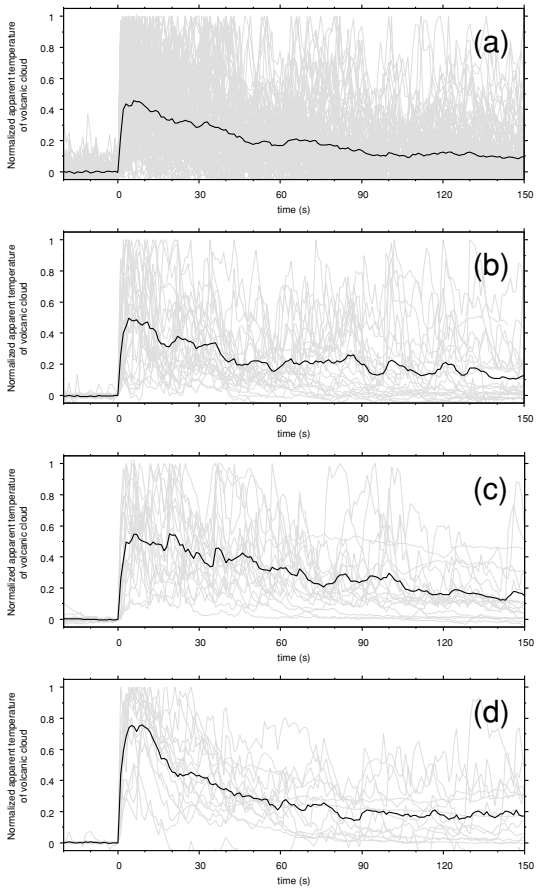

Fig. 5. Normalized temperature waveforms of volcanic clouds (gray lines) and stacked average responses (black lines). (a) 100 events with cloud temperature of 30–35°C, (b) 26 events with 50–55°C, (c) 19 events with 70–80°C, and (d) 16 events with >100°C (see also Fig. 4).

exit velocities.

When comparing the individual thermal waveforms of each eruption event, the stacked signals for temperature were estimated. That is, the maximum temperature was normalized to the background temperature immediately prior to the eruption (Harris and Thornber, 1999; Ripepe *et al.*, 2005) for the respective eruption events. Then, normalized waveforms classified by the maximum temperatures were stacked (Fig. 5). Although variations of more than 180°C in the maximum apparent temperature were recorded for individual events (Fig. 4), the stacked signals reveal the following common characteristics of the thermal waveforms, regardless of the individual temperatures; such as a rapid increase in temperature toward the peak value in the first 2–5 s, which is followed by a more gradual decrease over a few minutes, like the thermal waveforms observed at Santiaguito volcano (Sahetapy-Engel *et al.*, 2008).

The temporal changes in apparent cloud temperature for all recorded events in 2008 are displayed in Fig. 6. During the third eruption episode (February 3–6), a maximum cloud temperature of >250°C was recorded at the eruption with the largest PDC (Fig. 3(a)). This remains the highest temperature recorded at the Showa crater to date (May 2009). During this period, no distinct trend in temperatures could be identified, with considerable scattering over a wide temperature range (over 200°C) over just four eruptive days.

In the data for the fourth eruption episode, a decrease in the maximum cloud temperature seems to be recognized against a slight increase in the temperature minimum from April until August. The latter temperature change was dependent on an increase of ambient (background) temperature due to seasonal change from spring to summer. However, there were no other clear trends in the temperature

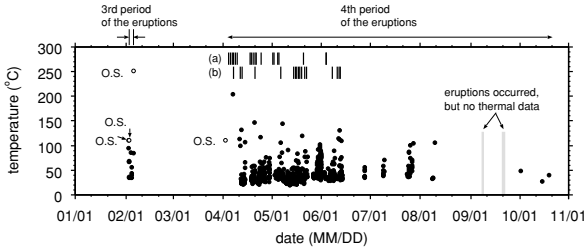

Fig. 6. Temporal change in apparent maximum temperature of volcanic clouds in 2008 (black circles). Four events could not be measured accurately due to over-scale readings (white circles labeled O.S.). Bars (a) and (b) indicate observed days of volcanic glow and eruptions with incandescent ejecta, respectively.

data due to large event-by-event fluctuations on each eruption day. Furthermore, no simple changes related to surface manifestation of eruptive activity described in Section 3, such as those observed in the second episode of eruptions in 2007 (Yokoo *et al.*, 2008b), were apparent for either the third or fourth eruption episodes. For example, eruption cloud temperatures over 100°C were observed from July to August when the activity became low, during which period there was neither volcanic glow nor reddish ejecta, which is recognized as simple evidence of the presence of high-temperature materials at a rather shallow portion of the crater. This suggests that it would be premature to con-

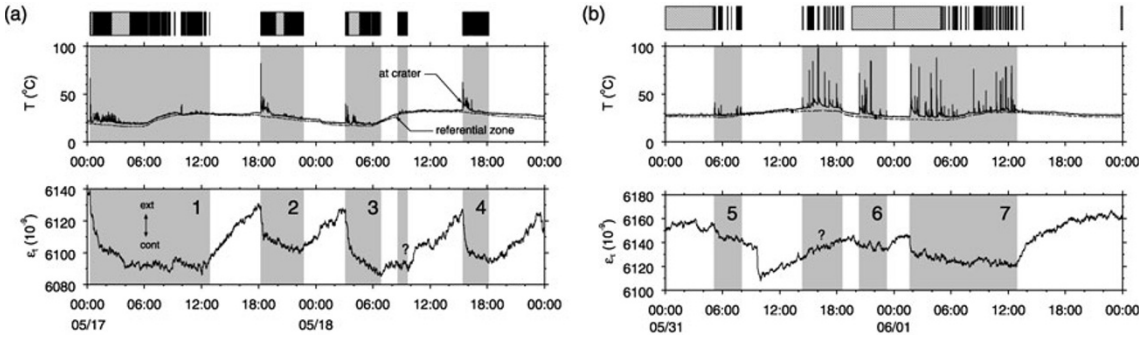

Fig. 7. Temporal relation among eruptive periods identified by visual observations (top; black solid), temperatures of volcanic cloud at the crater (analyzed zone in Fig. 2(a); solid line) referenced with average ground surface temperatures at normal area by a dotted line (upper diagram), and tangential component of strain changes in an underground tunnel at 2.2 km from the crater (lower diagram). Two 2-day periods are displayed in (a) May 17–18 and (b) May 31–June 1, with local time (UTC+9 h). The shading at the top of the diagrams denotes periods when the eruptive surface phenomena are obscured by the darkness of night or poor weather conditions. Up and down oscillations in the lower diagrams (ground deformation) represent extension and contraction, respectively.

sider relating observed temperatures of volcanic clouds to the progress of volcanic activity. It also means that any other factors controlling these temperatures need to be examined; e.g., size and volume fractions of hot particles in the cloud within the iFOV of the camera, which are affected by a fragmentation process of magma occurring within the conduit.

5. Released Radiative Thermal Energy

Figure 7 shows the temporal relation over 2-day periods among eruptive periods at the Showa crater identified by video images, cloud temperatures with referential ones that were both obtained by the thermal monitoring system, and the tangential component of the strain changes that were observed in an underground tunnel at 2.2 km from the crater. As Iguchi *et al*. (2008b) mentioned, strong relations between the surface manifestation and temporal changes of ground deformation, such as saw-tooth patterns, were sometimes recognized in the repeated eruptive periods during the 2008 episode (Fig. 7(a)). In contrast, less clear geodetic changes were observed during other periods of eruptions which were occurred continuously (Fig. 7(b)). Surface characteristics of each individual eruptive event were not quite different in both periods. The former type of geodetic pattern have been well reported and analyzed by many researchers (e.g., Ishihara, 1990; Iguchi *et al*., 2008a), however, the latter change has rarely been referenced, much less analyzed, because these patterns had been inconspicuous thus had not been identified previously.

For understanding the mass balance during eruptions with such clear or unclear geodetic records, estimation of the mass flux of the essential materials in grate detail is important but difficult (Ishihara, 1990). Alternatively the author focused the radiative heat energy of ejected volcanic cloud, which would be proportional to the mass of the essential materials during continuous eruptions. The radiative energy has been shown to be correlated with some eruptive parameters of ejected materials (Johnson *et al*., 2004; Scharff *et al*., 2008). Inevitably, here is evaluating whether the estimated thermal energies are correlated with the contracted volume of the ground.

Based on the volcanic cloud temperature T_{cloud} (K) in the findings of the current observation, the radiative thermal energy E (J) released in each eruption period i can be calculated by

$$E_i = \int^{\tau} \epsilon\sigma \cdot S(t) \cdot \left(T_{\mathrm{cloud}}^4 - T_{\mathrm{ref}}^4\right) \mathrm{d}t, \qquad (1)$$

according to Johnson *et al*. (2004) and Scharff *et al*. (2008), where ϵ is the emissivity (0.9), σ is the Stefan-Boltzmann constant (5.67×10^{-8} W·m^{-4} K^{-4}), $S(t)$ (m^2) is the area of the eruption cloud at the crater in the thermal data, T_{ref} (K) is the background temperature, and τ (s) is the duration of volcanic cloud venting from the crater.

Here, the value of T_{ref} is set to the average temperature of the nearest, non-anomalous thermal region around the crater (Fig. 2; Yokoo *et al*., 2007) in order to exclude diurnal changes due to ambient conditions (solar heating and cooling; Fig. 7) that overlap with observed temperatures. Moreover, the following two additional assumptions are considered for estimating a proxy for the energy E_i. One is that all ejected particles within an analyzed area are at almost the same temperature at each moment, and the other is that cloud area in the image just above the crater $S(t)$ is fixed with time. Accordingly, E_i becomes a simple function of $\int \left(T_{\mathrm{cloud}}^4 - T_{\mathrm{ref}}^4\right) dt$.

Figure 8(a) shows the log-log plot of resulting relation between volume changes associated with each eruptive period (gray masked periods in Fig. 7) that were estimated using strain and tilt changes assuming Mogi's model (Mogi, 1958; Ishihara, 1990) and proxy for radiative thermal energies estimated by Eq. (1). A weak, but positive, correlation is apparently observed. Although the data set is too small to establish any credible relation between radiative thermal energy and volume changes, it is confirmed that continuous ash emissions would be also related to the contraction of the magma chamber as of the distinct repeated eruptions. These proxy for the energies are essentially based on apparent temperatures, however, temperatures themselves are not surely correlated with the volume changes (Fig. 8(b)) because they lack information on each duration of eruptive period. Although some questions are still opened on these results, for example, about precise relation between ejected volume of the cloud and estimated volume change of contraction inferred from geodetic data at each event, like a

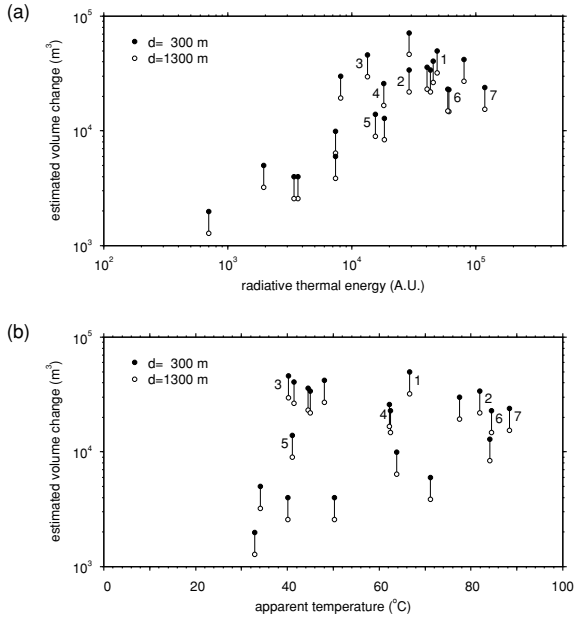

Fig. 8. (a) Relation between radiative energy proxy and estimated volume change associated with each eruptive period (21 periods, May 15–June 5). For the estimation, depths of contracting source were assumed to be 300 and 1300 m, respectively, beneath the crater (Iguchi, pers. comm.). Numbers of 1–7 correspond eruptive periods shown in Fig. 7. (b) Relation between maximum apparent temperatures and volume changes.

result of Ishihara (1990), the temperature data of volcanic clouds available from infrared thermal image monitoring will possibly become a useful key in appreciating the mass and energy balance during future eruptions.

6. Summary

Using a new thermal monitoring system installed to observe eruptions at the Showa crater of Sakurajima volcano, eruptions were found to exhibit an initial rapid increase in temperature, followed by a gradual cooling. All observed thermal waveforms captured at a sampling rate of 1 Hz were found to be quite similar, despite recording a wide range ($>180^{\circ}$C) of maximum cloud temperatures. Although comparison of these thermal data with other geophysical records (e.g., seismic and geodetic records) may have the potential to provide useful information for understanding the eruption mechanisms of volcanoes, the present thermal monitoring was not sufficient to clarify the changes in eruptive activity in 2008. Further refinement to utilize data obtained by the permanent thermal monitoring system and detailed thermodynamics of volcanic cloud for each eruption event at the Showa crater will be discussed on another occasion.

Acknowledgments. The author is grateful to M. Iguchi for supporting the present study and providing valuable comments and data on ground deformation, W. Kanda for provision of the thermal logging instrumentation, and colleagues at the Sakurajima Volcanological Observatory for their kind support. This work was funded in part by a JSPS Research Fellowship for Young Scientists (No. 19·126).

References

Chiodini, G., G. Valid, V. Augusti, D. Granieri, S. Caliro, C. Minopoli, and C. Terranova, Thermal monitoring of hydrothermal activity by permanent infrared automatic stations: Results obtained at Solfatara di Pozzuoli, Campi Flegrei (Italy), *J. Geophys. Res.*, **112**, B12206, doi:10.1029/2007JB005140, 2007.

Harris, A. J. L. and C. Thornber, Complex effusive events at Kilauea as documented by the GOES satellite and remote video cameras, *Bull. Volcanol.*, **59**, 49–64, 1999.

Harris, A. J. L., J. Johnson, K. Horton, H. Garbeil, H. Ramm, E. Pilger, L. Flynn, P. Mouginis-Mark, D. Pirie, S. Donegan, D. Rothery, M. Ripepe, and E. Marchetti, Ground-based infrared monitoring provides new tool for remote tracking of volcanic activity, *Eos*, **84**, 409–424, 2003.

Harris, A. J. L., L. Lodato, J. Dehn, and L. Spampinato, Thermal characterization of the Vulcano fumarole field, *Bull. Volcanol.*, **71**, 441–458, doi:10.1007/s00445-008-0236-8, 2009.

Iguchi, M., H. Yakiwara, T. Tameguri, M. Hendrasto, and J. Hirabayashi, Mechanism of explosive eruption revealed by geophysical observations at the Sakurajima, Suwanosejima and Semeru volcanoes, *J. Volcanol. Geotherm. Res.*, **178**, 1–9, doi:10.1016/j.jvolgeores.2007.10.010, 2008a.

Iguchi, M., A. Yokoo, and T. Tameguri, Characteristics of ground deformation associated with eruptions at Showa crater, Sakurajima volcano, *Abstr. Volcanol. Soc. Japan 2008 Fall Meet.*, B26, 2008b (in Japanese).

Ishihara, K., Pressure sources and induced ground deformation associated with explosive eruptions at an andesitic volcano: Sakurajima volcano, Japan, in *Magma Transport and Storage,* edited by M. P. Ryan, 336–356, 1990.

Johnson, J. B., A. J. L. Harris, S. T. M. Sahetapy-Engel, R. Wolf, and W. I. Rose, Explosion dynamics of pyroclastic eruptions at Santiaguito Volcano, *Geophys. Res. Lett.*, **31**, L06610, doi:10.1029/2003GL019079, 2004.

Kamo, K., K. Nishi, M. Iguchi, and T. Takayama, Observation of thermal anomaly area on the ground surface of flank of Minamidake, Sakurajima volcano, using an infrared thermal camera, in *The 8th joint observations of Sakurajima volcano*, 31–36, 1995 (in Japanese).

Kaneko, T., K. Takasaki, A. Yasuda, and Y. Aoki, Thermal surveillance of the Asama 2004–2005 activity using MODIS night-time infrared images, *Bull. Volcanol. Soc. Jpn.*, **51**, 273–282, 2006 (in Japanese with English Abstract).

Mogi, K., Relation between the eruptions of various volcanoes and the deformations of the ground surface around them, *Bull. Earthq. Res. Inst., Univ. Tokyo*, **38**, 99–134, 1958.

Patrick, M. R., A. J. L. Harris, M. Ripepe, J. Dehn, D. A. Rothery, and S. Calvari, Strombolian explosive styles and source conditions: insights from thermal (FLIR) video, *Bull. Volcanol.*, **69**, 769–784, doi:10.1007/s00445-006-0107-0, 2007.

Ripepe, M., A. J. L. Harris, and E. Marchetti, Coupled thermal oscillations in explosive activity at different craters of Stromboli volcano, *Geophys. Res. Lett.*, **32**, L17302, doi:10.1029/2005GL022711, 2005.

Sahetapy-Engel, S. T., A. J. L. Harris, and E. Marchetti, Thermal, seismic and infrasound observations of persistent explosive activity and conduit dynamics at Santiaguito lava dome, Guatemala, *J. Volcanol. Geotherm. Res.*, **173**, 1–14, 2008.

Scharff, L., M. Hort, A. J. L. Harris, M. Ripepe, J. M. Lees, and R. Seyfried, Eruption dynamics of the SW crater of Stromboli volcano, Italy—An interdisciplinary approach, *J. Volcanol. Geotherm. Res.*, **176**, 565–570, 2008.

Stevenson, J. A. and N. Varley, Fumarole monitoring with a hand-held infrared camera: Volcán de Colima, Mexico, 2006–2007, *J. Volcanol. Geotherm. Res.*, **177**, 911–924, doi:10.1016/j.jvolgeores.2008.07.003, 2008.

Yokoo, A., M. Iguchi, and K. Ishihara, Geothermal activity on the flank of Sakurajima volcano inferred from infrared thermal observation, *Bull. Volcanol. Soc. Jpn.*, **52**, 121–126, 2007 (in Japanese with English Abstract).

Yokoo, A., T. Tameguri, and M. Iguchi, Continuous monitoring of thermal activity around Showa crater of Sakurajima volcano with an infrared thermal camera, in *The 10th joint observations of Sakurajima volcano*, 113–122, 2008a (in Japanese).

Yokoo, A., T. Tameguri, M. Iguchi, and K. Ishihara, Sequence and characteristics of the 2007 eruptions at Showa crater of Sakurajima volcano, *Ann. Disas. Prev. Res. Inst.*, **51**, 267–273, 2008b (in Japanese with English Abstract).

Yokoo, A., T. Tameguri, and M. Iguchi, Swelling of a lava plug associated with a Vulcanian eruption at Sakurajima Volcano, Japan, as revealed by infrasound record: case study of the eruption on January 2, 2007, *Bull. Volcanol.*, **71**, 619–630, doi:10.1007/s00445-008-0247-5, 2009.

A. Yokoo (e-mail: yokoo@zisin.gp.tohoku.ac.jp)